Erzincan Üniversitesi
Fen Bilimleri Enstitüsü Dergisi
2023, 16(3), 615-632
ISSN: 1307-9085, e-ISSN: 2149-4584
Araştırma Makalesi

Erzincan University
Journal of Science and Technology
2023, 16(3), 615-632
DOI: 10.18185/erzifbed.1189339
Research Article

Investigation of Posaconazole Loading and Release Behavior in Surface-Modified Mesoporous Silica Nanoparticular System

Hilal ERKAN[1], Ceren KEÇECİLER-EMİR[1,2,3], Cem ÖZEL[1,3], Sevil YÜCEL[1,3*]

[1]Yildiz Technical University, Faculty of Chemical and Metallurgical Engineering, Department of Bioengineering, Istanbul, Turkey
[2]Alanya Alaaddin Keykubat University, Faculty of Rafet Kayis Engineering, Genetic and Bioengineering Department, Antalya, Turkey
[3] Health Biotechnology Joint Research and Application Center of Excellence, 34220 Esenler, Istanbul, Turkey

Received: 14/10/2022, **Revised**: 31/03/2023, **Accepted**: 02/04/2023**, Published**: 31/12/2023

Abstract

Posaconazole (PCZ) is an antifungal agent and its absorption is difficult due to its low solubility in aqueous and acidic environments leading low therapeutic effect and low bioavailability. Mesoporous silica nanoparticles (MSN) are biocompatible biomaterials that have a large surface area, high pore volume, and enhanced adsorption capacity. With MSN-mediated controlled drug release, the active substance concentration is kept within the desired therapeutic range. In this study, it is aimed to enhance the PCZ adsorption and release by using a MSN based drug delivery system. MSNs were synthesized by sol-gel method. Specific surface area and pore diameter of MSN was measured as 705.9 m^2/g and 3.33 nm, respectively. Surface modification of nanoparticles was achieved using (3-Aminopropyl) triethoxysilane (APTES). Zeta potential of APTES-modified MSN (MSN-NH_2) measured higher compared to zeta potential of MSN. PCZ was loaded on MSN-NH_2 with a loading efficiency of 35%. The release profile of PCZ from MSN-$NH_2$was observed as diffusion controlled release, and 19% of PCZ was released at the end of 16 hours. According to the MTT test, drug loaded MSN-NH2 showed cell viability greater than 90%.

Keywords: Antifungal, Drug delivery system, Nanoparticle, Posaconazole, Silica

Yüzeyi Modifiye Edilmiş Mezogözenekli Silika Nanopartiküler Sistemde Posakonazol Yüklenmesi ve Salım Davranışının İncelenmesi

Öz

Posakonazol (PCZ) bir antifungal ajandır ve sulu ve asidik ortamlarda düşük çözünürlüğü emilimi zordur ve bu da düşük terapötik etkiye ve düşük biyoyararlanıma yol açmaktadır. Mezogözenekli silika nanoparçacıkları (MSN), geniş bir yüzey alanına, yüksek gözenek hacmine ve gelişmiş adsorpsiyon kapasitesine sahip biyouyumlu biyomalzemelerdir. MSN aracılı kontrollü ilaç salımı ile kandaki etken madde konsantrasyonu istenilen terapötik aralıkta tutulmaktadır. Bu çalışmada, MSN tabanlı bir ilaç salım sistemi kullanılarak PCZ adsorpsiyonunun ve salımının arttırılması amaçlanmıştır. MSN'ler sol-gel yöntemiyle sentezlenmiştir. MSN'nin özgül yüzey alanı ve gözenek çapı sırasıyla 705,9 m^2/g ve 3,33 nm olarak ölçülmüştür. Nanoparçacıkların yüzey modifikasyonu, (3-Aminopropil) trietoksisilan (APTES) kullanılarak sağlanmıştır ve APTES ile değiştirilmiş MSN'nin (MSN-NH_2) zeta potansiyeli, MSN'nin zeta potansiyeline kıyasla daha yüksek olarak ölçülmüştür. PCZ, %35'lik bir yükleme verimliliği ile MSN-NH_2'ye yüklenmiştir. PCZ'nin MSN-NH_2'den salım profili difüzyon kontrollü salım olarak gözlenmiş ve 16 saat sonunda PCZ'nin %19'u salınmıştır. MTT testine göre, ilaç yüklü MSN-NH_2, %90'ın üzerinde hücre canlılığı göstermiştir.

Anahtar Kelimeler: Antifungal, İlaç taşıma sistemi, Nanopartikül, Posakonazol, Silika

***Corresponding Author:** syucel@yildiz.edu.tr
Hilal Erkan, https://orcid.org/0000-0002-3836-8850
Ceren Keçeciler-Emir, https://orcid.org/0000-0001-9015-3104
Cem Özel, https://orcid.org/0000-0002-6288-2091
Sevil Yücel, https://orcid.org/0000-0002-9495-9321

1. Introduction

The biggest challenge in medicine today is how to achieve successful treatment. In the conventional therapy, pure drugs can cause side effects resulting from non-specific uptake of the drug by healthy cells. This problem may result in a limitation of dose success in defective cells. Because of this, patients take higher doses of drugs that lack specificity and solubility to achieve adequate therapeutic effects, all of which also result in systemic toxicity [1]. In addition, many drugs with low water solubility or hydrophobicity make direct administration difficult [2]. All these factors decrease the efficiency of the active substance [3]. To respond to these challenges, controlled release systems are designed to increase the effectiveness of drugs used during treatment and are systems that prevent the physiological degradation of the drug in the body by ensuring that the desired effective dosage of the drug is delivered to the targeted cells [4]. Controlled release systems ensure a constant concentration of the therapeutic drug in the blood with minimal fluctuation, prevent the degradation of drugs with very short half-lifes, reduce the side effects of drugs, and make drugs more stable in the body. At the same time, controlled release systems decrease the frequency of drug administration due to the long-term reproducible release rate, and help ensure patient compliance [5].

Posaconazole (PCZ) is a novel antifungal agent which has antifungal activity against common fungal species and some endemic fungi. PCZ inhibits the enzyme lanosterol 14-alpha demethylase (CYP51), which catalyzes the essential step in ergosterol (the main component for fungal cell membrane) biosynthesis. Since PCZ is hydrophobic and exhibits low solubility in an aqueous and acidic environment, adsorption of PCZ is limited resulting in low bioavailability (Szekalska et al., 2019). According to Biopharmaceutical Classification System (BCS), PCZ is classified as a class II drug, which has low solubility and high lipophilicity properties (Mudie et al., 2020). Despite its broad spectrum, its high lipid solubility leads to difficulties in drug absorption. The use of controlled drug release systems avoids these problems and facilitates the absorption and release of PCZ [6].

Mesoporous silica nanoparticles (MSNs) have been frequently used as drug carriers since they have significant features such as being highly biocompatible, non-toxic nature, enhanced adsorption capacity, high surface area, and pore volume. Controlled drug release is also achieved by modifying the surface of MSNs. Hydroxyl groups (-OH) present on the surface of MSNs provide functionalization resulting in an increase in interactions between the drug and MSN, and thus the drug dosage is maintained at the desired level [7], [8].

Gounani et al. (2018) loaded polymyxin B and vancomycin antibiotics into unmodified MSNs, and carboxyl-modified MSNs to provide simultaneous local antibiotic delivery against gram-positive and gram-negative bacteria. Antibiotics have been reported to have synergistic effects against gram-negative bacteria. It was found that the antimicrobial efficacy of drug-loaded carboxyl-modified MSN was much higher than that of pure antibiotics. All these findings showed that the drug delivery systems increase the antimicrobial efficiency of antibiotics. These systems can be a good candidate for fighting infections and enhancing the antibiotic efficiency against gram-positive and gram-negative bacteria [9].

Ge et al. (2017) prepared doxorubicin (DOX)-loaded polydopamine (PDA)-modified MSNs for the bladder cancer treatment. CSNRDARRC (PEP) as a targeting peptide fragment was conjugated onto the PDA coating of MSN-PDA-DOX. In vitro drug release demonstrated that DOX-loaded MSN-PDA and MSN-PDA-PEP have similar DOX release profiles. At neutral pH, DOX molecules are easily trapped in MSNs. Drug release was reported as pH sensitive since DOX molecules are released at acidic environment by PDA coating. According to the results, ligand-receptor recognition of DOX-loaded MSN-PDA-PEP resulting much more efficient cellular uptake. Targeted DOX-loaded MSN-PDA-PEP nanocarriers have been shown to be significantly superior in antitumor effects to free DOX and DOX-loaded MSN-PDA [10].

Tiryaki et. al. (2020) coated inorganic silica aerogels with organic polymers dextran (Dex) and dextran aldehyde (Dex-CHO). Due to the secretion of dextranase enzyme in the colon, silica aerogels were coated with Dex and Dex-CHO and then used as a delivery system of the 5-Fluorouracil (5-FU) drug. To improve drug loading efficiency and coating, the silica aerogel surface was functionalized using APTES. Since the drug and amine groups has electrostatic interaction, silica aerogels coated with amine groups have been reported to load higher amounts of drug than unmodified silica aerogels. Release studies showed that the Dex and Dex-CHO coated silica aerogels can provide controlled release of 5-FU triggered by dextranase enzyme in the colon region without released in acidic pH in upper gastrointestinal tract. According to the results of MTT test, all silica aerogels without 5-FU have no cytotoxic effects on Caco-2 cell lines. Cell viability was decreased after 5-FU loading on silica aerogels [7].

The current study, it was aimed to enhance the loading and release of the hydrophobic drug PCZ by using hydrophilic MSN as a drug delivery system. MSNs were synthesized by the sol-gel method, and the surface of MSN was modified with APTES. PCZ was loaded on APTES-modified MSNs (MSN-NH2) and its controlled release in simulated gastric fluid (SGF) was investigated. The Electrophoretic Light Scattering (ELS) method was used to determine the zeta potential of MSN, MSN-NH2, and MSN-NH2-PCZ. Scanning Electron Microscopy (SEM) and Fourier-Transform Infrared Spectroscopy (FTIR) were performed for morphological and functional group analysis, respectively. The UV Spectrophotometer was used to determine drug loading efficiency and drug release profile. The surface area, pore volume, and pore size of MSN, MSN-NH2, and MSN-NH2-PCZ were measured using the Brunauer-Emmett-Teller (BET) and Barrett-Joiner-Halenda (BJH) methods. Cell viability tests of MSN, PCZ, and MSN-NH2-PCZ on L929 cell lines were performed by the MTT assay.

2. Material and Methods

2.1. Materials

Tetraethyl orthosilicate (TEOS, 98%), cetyl trimethyl ammonium bromide (CTAB, 99%), formaldehyde (37%) sodium hydroxide (NaOH), ammonium hydroxide (NH_4OH, 25–28%), sodium chloride (NaCl), and hydrochloric acid (HCl) were purchased from Merck (Germany). (3-Aminopropyl) triethoxysilane (APTES), dichloromethane (CH_2Cl_2), toluene, and ethanol (>99%) were purchased from Sigma-Aldrich (USA). Posaconazole (PCZ) was kindly supplied from Abdi İbrahim Pharmaceuticals (Turkey).

2.2. Synthesis of the MSN

MSN synthesis was achieved by sol-gel process [11]. 2.56 g of CTAB was dissolved in 40 mL of formaldehyde solution and stirred for 10 minutes on a magnetic stirrer. 11.2 mL of ammonia was added and ultrasonically mixed for 30 minutes. 11.2 mL of TEOS was added to the mixture and magnetically stirred for 2 hours. The resulting mixture was centrifuged (Nuve-Bench Top Centrifuge, NF 1200R, Turkey) and washed with ethanol for few times. After drying in vacuum (Vacucell, MMM, Germany) at 50°C, MSN was obtained by removing CTAB molecules at 500°C for 6 hours in a muffle furnace (Protherm Furnaces PLF110/6, Turkey).

2.3. Surface modification with APTES (MSN-NH_2)

Functionalization of the MSN was carried out by surface modification with APTES. MSN:APTES (w/v) ratio was determined as 1:10. Drying moisture balance device (Radwag, MA 50. R, Poland) was used for removing the moisture from nanoparticles. After the removal of moisture from the MSNs, 200 mg of MSN was ultrasonically dispersed in 20 mL of toluene. Then, 2 mL of APTES was added, and the reaction was carried out under reflux at 120°C for 24 hours. APTES-modified MSN (MSN-NH2**)** were obtained by centrifugation and washed with ethanol several times. The collected MSN-NH2 were dried at 80°C in a vacuum overnight [12].

2.4. Characterizations of the MSN

2.4.1. Scanning Electron Microscopy (SEM)

The morphological characteristics of the MSN, MSN-NH_2 and MSN-NH_2-PCZ were determined by utilizing an SEM (Carl Zeiss, EVO® Ls 10T, Germany). The instrument was performed at the accelerating voltage of 10 kV. Before characterization, all samples were covered with gold via a Sputter Coater device (Emitech K550X) under vacuum, and images were obtained for the analysis.

2.4.2. Fourier-Transform Infrared (FTIR) Spectroscopy

An IR spectrophotometer was used to record the FTIR spectra of the MSN, NH_2, and MSN-NH_2-PCZ for the multi-component system in the attenuated total reflection (ATR) mode (Thermo Fisher Co., USA). The IR spectra were generated using ten scans per sample, with a range of 4000 - 650 cm^{-1}.

2.4.3. Zeta Potential Measurements

Zeta potential measurements of the MSN, MSN-NH_2, and MSN- NH_2-PCZ were performed by Electrophoretic Light Scattering (ELS) method using a Zetasizer device (Nano ZS, Malvern Instruments, GB). Before the measurement, samples were ultrasonically dispersed in distilled water (pH 6.5) at a concentration of 0.05 mg/mL.

2.4.4. Specific Surface Area and Porosity Measurements

All samples were analyzed by using a surface area and pore size distribution analyzer (Micromeritics Instrument Corp., TriStar II 3020, USA) at 77 K to determine specific surface area, pore size, and pore volume. To prepare the samples for N2 adsorption, MSN and MSN-NH_2 were degassed at 200°C for 6 h, MSN- NH_2-PCZ sample was degassed at 100°C for 6 h (for preventing PCZ decomposition) under nitrogen to remove any moisture and adsorbed gas (Zaharudin et al., 2020), (Basaran Elalmis et al., 2021). The Brunauer–Emmett–Teller (BET)

and Barrett–Joiner–Halenda (BJH) methods were used for estimating the specific surface area, and pore volume of the samples, respectively. The pore size distributions were obtained from generated adsorption isotherms.

2.5.Drug Loading Studies

To load PCZ into MSN-NH_2, PCZ was first dissolved in DCM resulting in the concentration of 4 mg/mL drug solution. 60 mg of MSN-NH_2 was dispersed in 4.5 mL of drug solution on the ultrasonicator for 30 minutes. To provide maximum drug loading in the MSN channels, the mixture was stirred on a magnetic stirrer for 24 hours at 500 rpm. After centrifugation, MSN-NH_2-PCZ were collected and dried overnight at 40°C in a vacuum [13], [14].

In order to evaluate the loading efficiency (LE) of MSN-NH_2, supernatant was kept after drug loading study. UV Spectrophotometer (Scinco, S-3100, Korea) was utilized for absorbance measurement of remaining PCZ in the supernatant at 260 nm. The total PCZ concentration in MSN-NH_2-PCZ was calculated from the calibration curve. The LE was determined using Equation 1 [15].

$$LE\ (\%) = \frac{total\ amount\ of\ PCZ - total\ amount\ PCZ\ in\ supernatant}{total\ amount\ of\ PCZ} \times 100 \qquad (1)$$

2.6. *In Vitro* Drug Release Studies

To evaluate the PCZ release from MSN-NH_2-PCZ, a release study was performed in simulated gastric fluid (SGF) at 37°C. 10 mg of PCZ-loaded MSN-NH_2 was dispersed in 3 mL of SGF in a cellulose dialysis membrane (Sigma, Germany), and the dialysis membrane was placed in a falcon tube containing 37 mL of SGF and started to agitation at 37°C and 130 rpm in a shaking incubator. 1 mL of the release medium was withdrawn for absorbance measurements, and 1 mL of fresh release medium was added after each measurement. The amount of PCZ present in the medium was determined by measuring absorbance by using a UV spectrophotometer at 260 nm [13], [14].

2.7. Drug Release Kinetics

Various kinetic models are used to verify the drug release efficiency of drug formulations and to determine the drug release profile. While developing controlled drug release systems, the selection of the appropriate mathematical model helps us to get information about the release profile of the drug from the nanoparticular delivery system, and how it will be transferred to the cells through a transfer mechanism in the body [16]. In this study, the PCZ release data from MSN-NH_2 were fitted by using various kinetic models. The kinetic models and their equations are given in Table 1 [17].

Table 1. Equations of kinetic models

Kinetic Model	Equation
Zero Order	$Q_t = Q_0 + K_0 t$

First Order	$lnQ_t = lnQ_0 + K_1 t$
Higuchi	$Q_t = K_H\sqrt{t}$
Korsmeyer -Peppas	$\frac{Q_t}{Q_\infty} = K_{KP} t^n$

Q_0 and Q_t represent the initial amount of PCZ in the release medium and the amount of PCZ released at a certain time, respectively. Q_t /Q_∞ indicates the fractional release of the drug. K_0, K_1, K_H, and K_{KP} are constants of the zero order, first order, Higuchi, and Korsmeyer-Peppas models, respectively. *n* value represents the diffusional exponent [17]. The n value determines the release mechanism of the drug from the nanoparticular systems. Since the n value is equal to or lower than 0.45, it is indicated that the drug release follows Fickian diffusion. If the n value is between 0.45 and 0.89, that means the release follows Non-Fickian diffusion. If the n value is 0.89, the release mechanism is case II transport; in case of n value is greater than 0.89, the release mechanism is super case II transport [18].

2.8. *In Vitro* Cytotoxicity Test

"ISO 10993-5: 2009-Biological evaluation of medical devices - Part 5: In vitro cytotoxicity tests" was used as the test protocol. According to this test, which is based on measuring the viability of cells through metabolic activity; The yellow MTT is metabolically reduced in living cells to a blue-violet formazan. The color intensity obtained because of colorimetric measurements performed after formazan is dissolved in alcohol is directly associated with the number of viable cells. L929 mouse fibroblast cells without mycoplasma, recommended in the standard, were used as the cell line. MTT, Dulbecco's modified Eagle's medium (DMEM), fetal bovine serum (FBS), penicillin-streptomycin, PBS, DAPI were purchased from Sigma-Aldrich. At 37°C with 5% CO_2, L929 cells were cultured in DMEM containing 10% FBS and 0.1% penicillin-streptomycin. Cells were separated from the culture plate with a confluence of 70%. Then, cells were resuspended in culture medium, and the cell suspension adjusted to 1 x 10^5 cells/mL. 100 µL of a cell suspension of 1×10^5 cells/mL was dispensed into the peripheral wells of a 96-well tissue culture plate. Cells were then incubated for 24 hours for allowing the formation of a monolayer on the flask. After incubation for a day, the culture medium was separated from the cells. 100 µL negative control (DMSO), positive control (medium), sample at decreasing concentrations (100%-80-60-50-40-20-10-5) from 0.2 g/mL extraction liquid extracts were added per well. Then, cells were incubated for 24 hours at 5% CO_2, 37 °C, >90% humidity conditions. Then, the culture medium was separated from the plates and washed with PBS. The test wells were then filled with 50 µL of MTT solution (5 mg/mL), and the plates underwent an additional 2-hour incubation period at 37°C. Following the removal of the MTT solution, 100 µL of DMSO was added to each well, and the plate was then transferred to a microplate reader with a 570 nm filter for measuring the absorbance with a reference wavelength of 650 nm. In order to calculate relative cell activity (BHA), the results of the materials were compared with untreated cells which are control experiments.

3. Result and Discussion

MSNs were synthesized by sol-gel method based on hydrolysis and condensation reactions of TEOS as a silica precursor in solution that was prepared in a basic environment. To obtain a uniform mesoporous structure, CTAB was used as a structure modifier. CTAB micelles formation was achieved by the dissolution of CTAB in formaldehyde solution. After TEOS was added dropwise to the solution, solvent molecules attached to the alkoxide causing nucleophilic substitution of the alkoxy group with a hydroxyl group. Consequently, the silanol (Si-OH) group was formed (Shchipunov, 2008). The hydrolysis step of silanes in the reaction environment led to the formation of reactive silonates (≡Si-O^-) [20]. Negatively charged reactive silanolates were electrostatically attracted to positively charged CTAB micelles, thus leading to a templating effect. These silonates condensed with other silanes to form siloxane (Si-O-Si) groups [21]. Finally, the mesoporous structure was obtained after removal of CTAB molecules by calcination.

The surface modification of MSNs was achieved with APTES. Toluene was used as a solvent, and MSNs were dissolved ultrasonically in toluene. After adding APTES to the solution, the reaction continued under reflux. Since silanol (Si-OH) groups were still present on the MSN surface, APTES molecules attacked to the silanol groups and MSN-NH_2 surface was coated with amine groups.

3.1. Scanning Electron Microscopy (SEM)

The surface texture and morphology of all MSN samples are shown in SEM images. As it can be seen in Figure 1, all samples are uniformly spherical shape, and the particles are homogeneously distributed with approximate particle diameter of 50 to 60 nm, although they are in agglomeration. This may be an implication of high surface area which leads to encouraging adherence of the PCZ drug [22]. The agglomeration results may also come from low zeta surface potential of samples. After successful functionalization of the MSNs with APTES and PCZ loading, no significant difference observed in particle sizes. The similar results were found in previous literature [23].

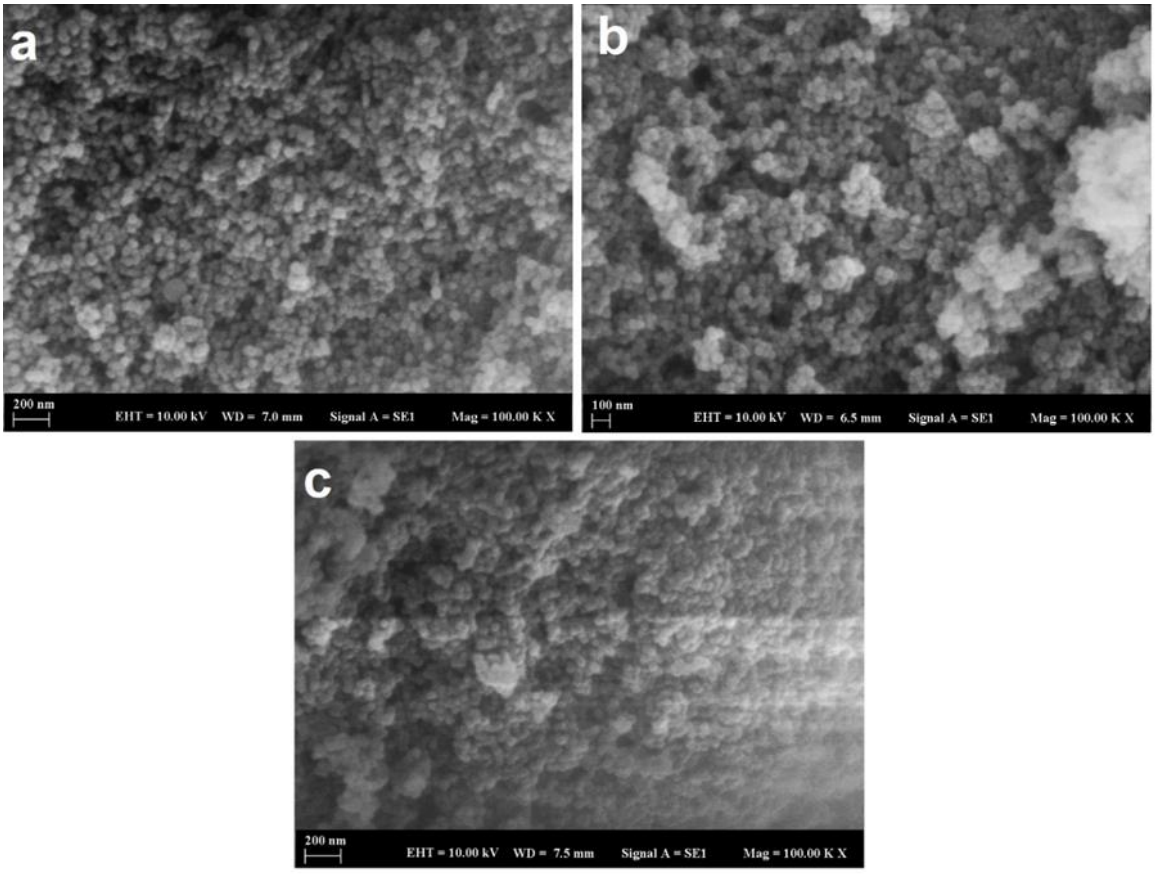

Figure 1. SEM images of (a) bare MSN, (b) MSN-NH_2 and (c) MSN-NH_2-PCZ

3.2. Fourier Transform Infrared (FTIR) Spectroscopy

The FTIR spectra given in Figure 2 show the characteristic peaks of MSN, MSN-NH_2 and MSN-NH_2-PCZ. In the spectrum of MSN with CTAB, the peaks of C-H stretching vibration of CTAB were seen at 2920 and 2880 cm^{-1}. The Si-O bond stretch of the surface Si-OH groups is shown at 960 cm^{-1}. In addition to the characteristic H-OH water bending band seen at 1640 cm^{1}, a broad hydroxyl stretching band was clearly seen moisture hydroxyls (-OH) at 3500 cm^{-1}. Also, the internal Si-O-Si stretching vibration of the SiO_4 asymmetric band was shown at 1100 cm^{-1} and the symmetrical one at 800 cm^{-1}. The silicate network is composed of Si-O-Si and abundant silanol (Si-OH) groups (both inner and outer). The peaks in the FTIR spectrum prove that MSN has been successfully synthesized.

The strong peaks observed in MSN at 800, 959, 1090 cm^{-1} are due to stretching vibrations of Si-O-Si, Si-OH. The vibration peaks of 1642 and 2953 cm^{-1}, represent amino groups. The O–H stretching vibration was seen at 568 and 3411 cm^{-1}. It was confirmed by FTIR spectrum analysis that it coincided with the peaks seen individually for MSN and MSN-NH_2. At 801, 953 and 1094 cm^{-1}, silica nanoparticles showed similar strong and distinct peaks. The N-H or O-H stretching vibration was seen as a broad peak at 3632 cm^{-1}. Nonetheless, the N-H peaks in the MSN-NH_2 sample were seen to remain very weak. The characteristic FTIR peaks of CTAB were given as N-H stretch at 3017 cm^{-1}, C-H stretch at 2918 and 2849 cm^{-1}, and C-N stretch at 1487 and 1462 cm^{-1}. It was confirmed by FTIR that these peaks of CTAB were not seen in the spectrum, thus removing CTAB from MSN by calcination.

The IR spectra showed the specific peaks associated with PCZ; =C-H and CH_2 stretching vibration was observed at 3979 cm^{-1}, and 3323 cm^{-1}; due to saturated ketone, C=O stretch was seen at 1651 cm^{-1}; and stretching of C=O-NH was observed at 1631 cm^{-1}. [24], [6], [25].

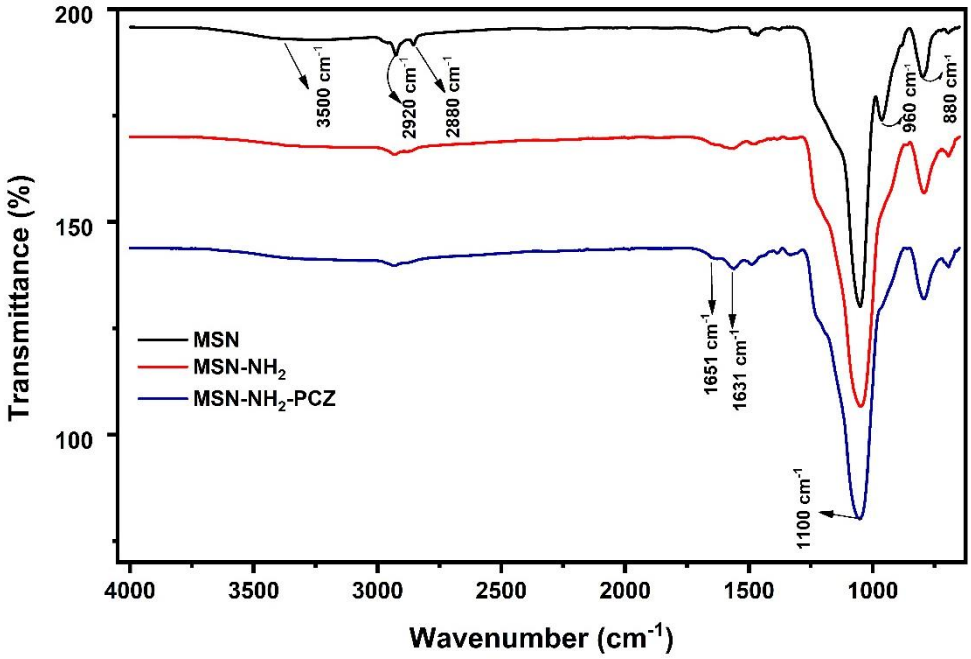

Figure 2. FTIR spectrum of MSN, MSN-NH_2 and MSN-NH_2-PCZ

3.3. Zeta Potential

Zeta potential of MSN, MSN-NH_2, and MSN-NH_2-PCZ was evaluated at 6.5 pH as shown in Table 3. Since surface of the MSN contains hydroxyl groups (-OH), its zeta potential was measured as a negative value. After surface modification, APTES molecules reacted with silanol groups (Si-OH) on the MSN surface, and the surface was coated with positive amine groups [7]. Thus, zeta potential of MSN-NH_2 became less negative compared to zeta potential of MSN. PCZ is a negatively charged molecule due to the carboxyl groups on its surface, and therefore, it was observed that the zeta potential of MSN-NH_2-PCZ increased after drug loading [26].

Table 3. Zeta potential values of MSN, MSN-NH_2, and MSN-NH_2-PCZ

	MSN	MSN-NH_2	MSN-NH_2-PCZ
Zeta potential (mV)	-5.86	-2.60	- 4.04

3.4. Specific Surface Area and Porosity Measurements

N_2 adsorption/desorption findings in the Table 4 reveal that the MSN sample has a high specific surface area and a large pore volume, which is coherent with previous research [27], [28], [29]. MSN and MSN-NH_2 have specific surface areas of 705.9 and 110.4 m^2/g, respectively. The N_2 adsorption/desorption isotherms of MSN, MSN-NH_2, and MSN-NH_2-PCZ samples were shown

in Figure 3. The largest number of N_2 gas adsorbed on porous solid materials is clearly dependent on the volume of pores present in the solid substance [30]. The results indicated that MSN had the largest amount of N_2 gas adsorbed at a relative pressure of 0.99. This was caused by the pores of the MSN having the largest pore volume (0.384 cm^3/g) compared with MSN-NH_2 and MSN-NH_2-PCZ. Figure 4 displays the pore size distribution (PSD) curves of the samples. According to the IUPAC classification, all MSN samples were in the mesoporous region [31]. All samples including MSN-NH_2-PCZ have a uniform PSD with a mean pore diameter of between 3.33 and 6.86 nm which indicates the MSN samples keep their mesoporous structure after APTES modification and PCZ loading. Lower values for surface area and pore volume and higher values for pore size were seen after treatment with APTES. The addition of organic functional groups (NH_2) with a higher molecular weight than hydroxyl groups reduces the surface area of silica aerogel particles. Because organic functional groups repel more strongly than hydroxyl groups, pore size increases following APTES modification [7]. There is no difference between MSN-NH_2 and MSN-NH_2-PCZ. MSN-NH_2 and MSN-NH_2-PCZ appear to have a broader PSD compared with bare MSN. This could be dedicated to the surface modification given by APTES preventing the MSN pore structure from collapsing as a result of increased capillary pressure.

The hysteresis loop geometry in the N_2 adsorption-desorption isotherms is determined by pores present in the material. All samples exhibited type IV isotherm, which confirms the typical properties of mesoporous materials (Figure 4) according to the IUPAC classification [31]. All samples exhibited an H1 type hysteresis loop that display well-defined cylindrical shape pore structures. Hysteresis loops of the MSN-NH_2 and MSN-NH_2-PCZ samples were identical, confirming that the pore shape was unaffected by APTES modification or PCZ loading, and their pore size was determined as mesoporous. [32].

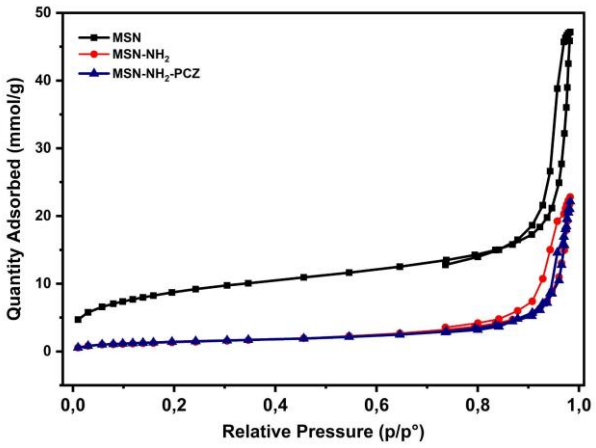

Figure 3. N_2 adsorption/desorption isotherms of the MSN, MSN-NH_2, and MSN-NH_2-PCZ

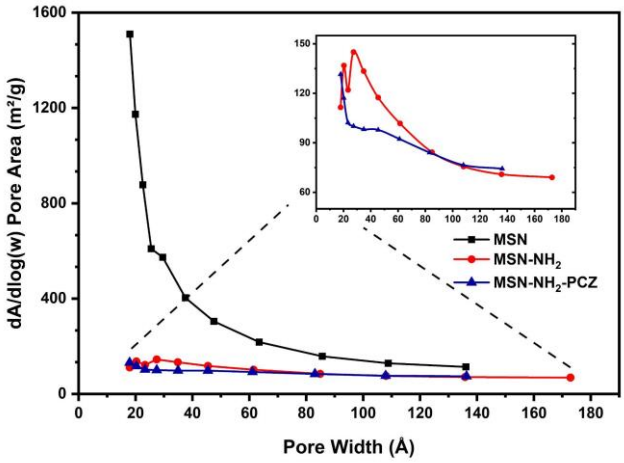

Figure 4. Cumulative pore size distributions of the MSN, MSN-NH_2, and MSN-NH_2-PCZ

Table 4. Textural properties of synthesized MSN, MSN-NH_2, and MSN-NH_2-PCZ

Sample	BET Specific Surface Area, (m^2/g)	BJH Pore Volume, (cm^3/g)	BJH Mean Pore Diameter, (nm)
MSN	705.9 ± 5.2	0.384	3.33
MSN-NH_2	110.4 ± 0.5	0.171	6.86
MSN-NH_2-PCZ	116.0 ± 1.2	0.127	6.2

3.5. Loading Efficiency, *In vitro* Drug Release and Mechanism

In order to evaluate the loading efficiency (LE) of MSN-NH_2, UV Spectrophotometer was used for absorbance measurement of unbound PCZ. The total amount of PCZ was calculated using a calibration curve with a correlation coefficient of R^2=0.996. Drug loading studies of PCZ in the literature showed loading efficiency between 30% and 46% [33]. In this study, drug loading efficiency was calculated as 35% which is compatible with the literature.

According to Tiryaki et al. (2020), after the surface modification with amino groups, the positively charged NH_2 groups present on the surface of the silica aerogel and the negatively charged hydrophobic drug interacted electrostatically to increase the silica aerogels' ability to bind drugs. Due to the negative charge of the Si-OH groups on the silica surface, it was observed to exhibit lower drug loading efficiency than the amine-modified ones [7]. The adsorption of PCZ molecules on MSN results the hydrogen bond formation. The surface of MSN-NH_2 is coated with positively charged amino groups. Therefore, PCZ, which is negatively charged at neutral pH values, could be electrostatically interacted with the surface of the MSN-NH_2 [26].

To investigate the release behaviour of PCZ from MSN-NH_2-PCZ, SGF was used as a release medium with pH of 1.2. MSN-NH_2-PCZ was placed in the dialysis membrane, and agitated at

37°C. At certain time intervals, absorbance measurement was performed by UV spectrophotometer. The amount of PCZ in the release medium was determined using UV spectrophotometer at 260 nm.

The results of release study showed that 7.2% PCZ was released from MSN-NH_2-PCZ in the first hour (Figure 5a). The fast release occurred during the first 2 hours with initial burst effect, and 12% PCZ was released at the end of the 3 h. Following the initial burst effect, a slower, sustained, and controlled release was observed. The release reached 14.5% at 4 h, and 19% PCZ was released after 16 h.

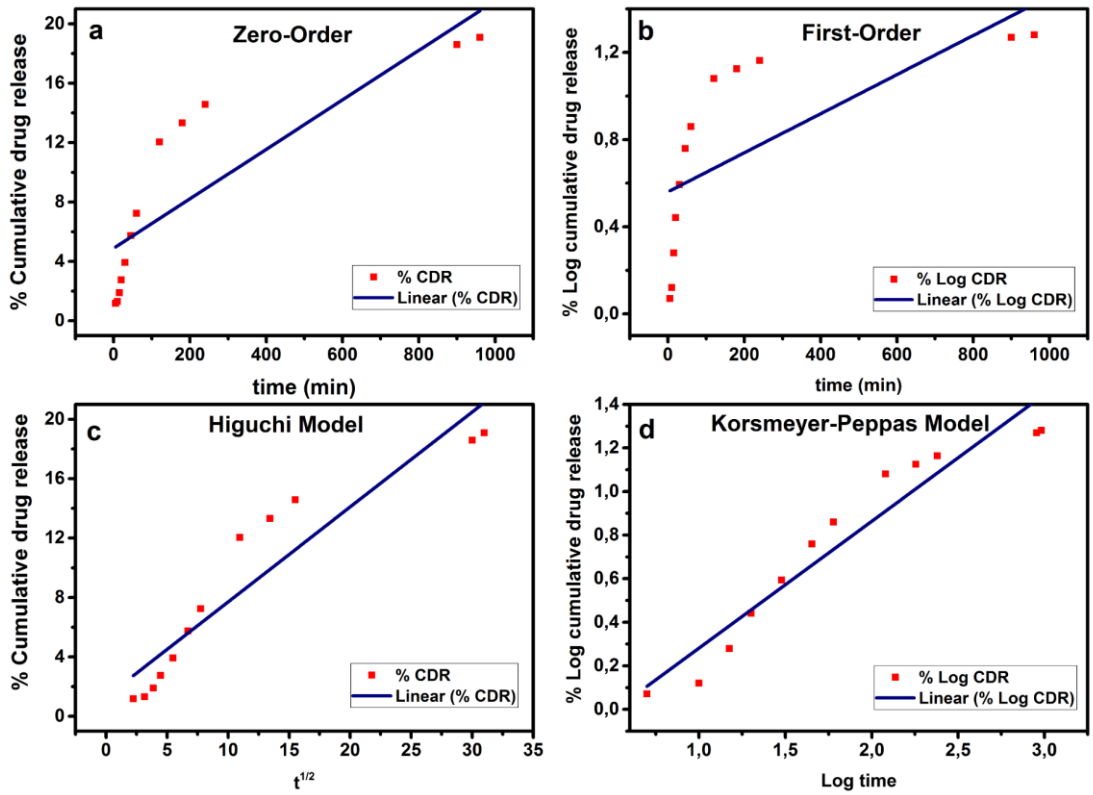

Figure 5. Release kinetics of PCZ from MSN-NH_2-PCZ

Table 5. PCZ release parameters obtained from various kinetic models

	Zero-Order	First-Order	Higuchi Model	Korsmeyer-Peppas Model
K	0.016	0.001	0.639	0.641
R^2	0.714	0.533	0.882	0.978
n	-	-	-	0.389

To investigate the release kinetics and release mechanism of PCZ from MSN-NH_2-PCZ, the resulting release values were fitted to zero-order, first-order, Higuchi and Korsmeyer-Peppas

kinetic models. Graphs were generated from the obtained data (Figure 5), and the correlation coefficient (R^2) of the graphs and rate constants were calculated (Table 5). According to the R^2 value of each model, it was determined that the release of PCZ more closely matched the Korsmeyer-Peppas kinetics. Drug release mechanism of Korsmeyer-Peppas model is determined by n value. In this study, n value was found as 0.389. Since n value is lower than 0.45, it is indicated that the PCZ release mechanism from MSN-NH_2-PCZ follows Fickian diffusion mechanism [18]. It was estimated that, due to the hydrophilicity of the silica pore walls, hydrophobic PCZ loaded on MSN is efficiently desorbed from the porous surface by competing adsorption with water molecules, and subsequently diffuses into the release media. [14].

3.6. *In vitro* Cytotoxicity

According to the procedure of "ISO 10993-5: 2009-Biological evaluation of medical devices - Part 5: In vitro cytotoxicity", the material is interpreted as having "cytotoxic potential" when the viability is >70% relative to the blank well. Test sample viability at 50% of applied concentration should be at least equal to or greater than 100% [34]. *In vitro* cytotoxicity test results are given in Figure 6. According to MTT test results; The cytotoxicity results of MSN, PCZ, and MSN-NH_2-PCZ on cells were above 70% viability compared to the positive control group. In this case, it was revealed that the NPs and the drug produced did not have any cytotoxic effect.

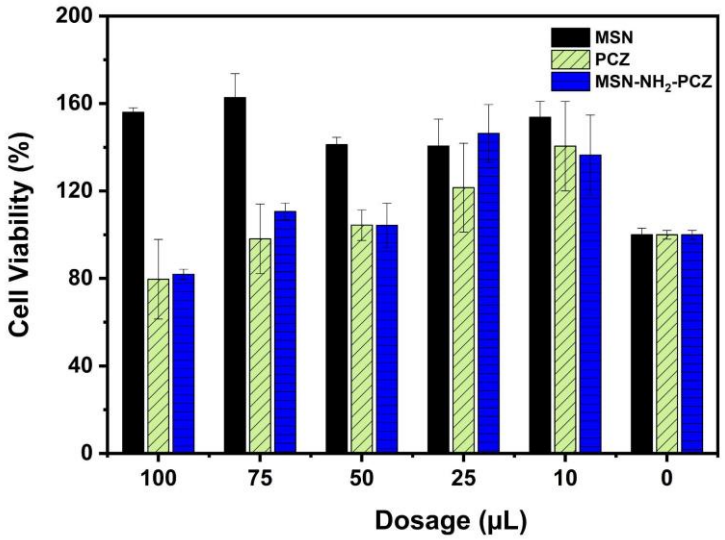

Figure 6. The cell viability results of MSN, PCZ and MSN-NH_2-PCZ on L929 cell line.

As an *in vitro* model and tool, L929 fibroblasts are used in various standard experiments, for example to test the biocompatibility of materials. Using an MTT test, Follmann et al. (2018) assessed the cell viability of L929 fibroblast cells after being exposed to MSNs for 72 hours at a 200 g/mL concentration. Cell viability in the presence of samples was found to be identical to that of the control group, according to the results of investigations on cell proliferation. All of the samples showed greater than 90% cell viability (approximately 93.5% on average). They

are suitable for a sustained, long-term drug delivery system since they are biocompatible and exhibit cell proliferation qualities comparable to controls. These results suggest that MSNs are good candidates for controlled release systems of drugs [35].

Mercorelli et al. (2020) reported that there was no cytotoxic effect of PCZ at concentrations up to 250 μM on the human foreskin fibroblast cell line. The cytotoxic effect of the maximum dose of PCZ loaded into the MSN and the concentrations below this dose were studied and no cytotoxic effect was observed in parallel with the data of this study [36].

4. Conclusion

In the current study, it was aimed to load the PCZ into MSN-NH_2 and facilitate its adsorption and release. MSNs were synthesized via the sol-gel method. The synthesized MSNs had a uniform spherical shape with a small size, high surface area, and negative surface zeta potential. MSNs were successfully functionalized by modification with APTES. After functionalization, the MSN surface was coated with positive amine groups, and zeta potential was decreased. 35% of PCZ was loaded onto MSN-NH_2 with electrostatic interactions since PCZ has a negative charge. In the release study, it was observed that 19% of PCZ was released at the end of 16 hours. Release kinetics of PCZ from MSN-NH_2-PCZ determined the release mechanism as Fickian diffusion. The cytotoxicity studies showed that the MSN-NH_2-PCZ has no cytotoxic effect. According to these results, PCZ-loaded MSNs may be a promising candidate to enhance the adsorption and release of PCZ and can be served as a controlled release system in the treatment of antifungal diseases.

Ethics in Publishing

There are no ethical issues regarding the publication of this study.

Author contributions

The authors did not declare any contributions.

Acknowledgments

This work has been supported by Yildiz Technical University Scientific Research Projects Coordination Unit under project number FYL-2021-4105. Cem ÖZEL also thanks the financial support from the Scientific and Technological Research Council of Turkey (TUBITAK) under the BIDEB/2211-A Doctoral Domestic Success Scholarship Program with project number 1649B032000005. The author(s) would like to acknowledge Assoc. Prof. Dr. Serap Derman for providing zeta analysis.

References

[1] Kwon, S., Singh, R.K., Perez, R.A., Neel, E.A.A., Kim, H.W., and Chrzanowski, W. (2013) Silica-based mesoporous nanoparticles for controlled drug delivery. Journal of Tissue Engineering. 4 (1), 1–18.

[2] Rosenholm, J.M., Sahlgren, C., and Lindén, M. (2010) Towards multifunctional, targeted drug delivery systems using mesoporous silica nanoparticles - Opportunities & challenges. Nanoscale. 2 (10), 1870–1883.

[3] Yan, L., Zhang, J., Lee, C.S., and Chen, X. (2014) Micro- and nanotechnologies for intracellular delivery. Small. 10 (22), 4487–4504.

[4] Slowing, I.I., Vivero-Escoto, J.L., Wu, C.W., and Lin, V.S.Y. (2008) Mesoporous silica nanoparticles as controlled release drug delivery and gene transfection carriers. Advanced Drug Delivery Reviews. 60 (11), 1278–1288.

[5] Bajpai, A.K., Shukla, S.K., Bhanu, S., and Kankane, S. (2008) Responsive polymers in controlled drug delivery. Progress in Polymer Science (Oxford). 33 (11), 1088–1118.

[6] Santana, A.C.S.G.V., Nadvorny, D., da Rocha Passos, T.D., de La Roca Soares, M.F., and Soares-Sobrinho, J.L. (2019) Influence of cyclodextrin on posaconazole stability, release and activity: Improve the utility of the drug. Journal of Drug Delivery Science and Technology. 53.

[7] Tiryaki, E., Başaran Elalmış, Y., Karakuzu İkizler, B., and Yücel, S. (2020) Novel organic/inorganic hybrid nanoparticles as enzyme-triggered drug delivery systems: Dextran and Dextran aldehyde coated silica aerogels. Journal of Drug Delivery Science and Technology. 56.

[8] Slowing, I.I., Trewyn, B.G., Giri, S., and Lin, V.S.Y. (2007) Mesoporous silica nanoparticles for drug delivery and biosensing applications. Advanced Functional Materials. 17 (8), 1225–1236.

[9] Gounani, Z., Asadollahi, M.A., Pedersen, J.N., Lyngsø, J., Skov Pedersen, J., Arpanaei, A., et al. (2019) Mesoporous silica nanoparticles carrying multiple antibiotics provide enhanced synergistic effect and improved biocompatibility. Colloids and Surfaces B: Biointerfaces. 175 498–508.

[10] Wei, Y., Gao, L., Wang, L., Shi, L., Wei, E., Zhou, B., et al. (2017) Polydopamine and peptide decorated doxorubicin-loaded mesoporous silica nanoparticles as a targeted drug delivery system for bladder cancer therapy. Drug Delivery. 24 (1), 681–691.

[11] Gu, L., Zhang, A., Hou, K., Dai, C., Zhang, S., Liu, M., et al. (2012) One-pot hydrothermal synthesis of mesoporous silica nanoparticles using formaldehyde as growth suppressant. Microporous and Mesoporous Materials. 152 9–15.

[12] He, Y., Luo, L., Liang, S., Long, M., and Xu, H. (2017) Amino-functionalized mesoporous silica nanoparticles as efficient carriers for anticancer drug delivery. Journal of Biomaterials Applications. 32 (4), 524–532.

[13] Liu, X. and Che, S. (2015) Enhanced release of the poorly soluble drug itraconazole loaded in ordered mesoporous silica. Science China Chemistry. 58 (3), 400–410.

[14] Ren, X., Cheng, S., Liang, Y., Yu, X., Sheng, J., Wan, Y., et al. (2020) Mesoporous silica nanospheres as nanocarriers for poorly soluble drug itraconazole with high loading capacity and enhanced bioavailability. Microporous and Mesoporous Materials. 305.

[15] Gomes, M.J., Martins, S., Ferreira, D., Segundo, M.A., and Reis, S. (2014) Lipid nanoparticles for topical and transdermal application for alopecia treatment: Development, physicochemical characterization, and in vitro release and penetration studies. International Journal of Nanomedicine. 9 (1), 1231–1242.

[16] Lisik, A. and Musiał, W. (2019) Conductomeric evaluation of the release kinetics of active substances from pharmaceutical preparations containing iron ions. Materials. 12 (5),.

[17] Costa, P., Manuel, J., and Lobô´´, S. (2001) Modeling and comparison of dissolution profiles. .

[18] Salah Eldeen, T., Ahmed, L., Atif, R., Yahya, I., Omara, A., and Eltayeb, M. (2019) Study the Using of Nanoparticles as Drug Delivery System Based on Mathematical Models for Controlled Release. .

[19] Shchipunov, Y.A. (n.d.) 3 Entrapment of Biopolymers into Sol-Gel-derived Silica Nanocomposites. .

[20] Croissant, J.G., Fatieiev, Y., Almalik, A., and Khashab, N.M. (2018) Mesoporous Silica and Organosilica Nanoparticles: Physical Chemistry, Biosafety, Delivery Strategies, and Biomedical Applications. Advanced Healthcare Materials. 7 (4),.

[21] Yang, B., Chen, Y., and Shi, J. (2019) Mesoporous silica/organosilica nanoparticles: Synthesis, biological effect and biomedical application. Materials Science and Engineering R: Reports. 137 66–105.

[22] Ebisike, K., Okoronkwo, A.E., and Alaneme, K.K. (2020) Synthesis and characterization of Chitosan–silica hybrid aerogel using sol-gel method. Journal of King Saud University - Science. 32 (1), 550–554.

[23] Zaharudin, N.S., Mohamed Isa, E.D., Ahmad, H., Abdul Rahman, M.B., and Jumbri, K. (2020) Functionalized mesoporous silica nanoparticles templated by pyridinium ionic liquid for hydrophilic and hydrophobic drug release application. Journal of Saudi Chemical Society. 24 (3), 289–302.

[24] Mudie, D.M., Stewart, A.M., Biswas, N., Brodeur, T.J., Shepard, K.B., Smith, A., et al. (2020) Novel High-Drug-Loaded Amorphous Dispersion Tablets of Posaconazole; in Vivo and in Vitro Assessment. Molecular Pharmaceutics. 17 (12), 4463–4472.

[25] Danda, L.J. de A., Batista, L. de M., Melo, V.C.S., Soares Sobrinho, J.L., and Soares, M.F. de L.R. (2019) Combining amorphous solid dispersions for improved kinetic solubility of posaconazole simultaneously released from soluble PVP/VA64 and an insoluble ammonio methacrylate copolymer. European Journal of Pharmaceutical Sciences. 133 79–85.

[26] Figueirêdo, C.B.M., Nadvorny, D., de Medeiros Vieira, A.C.Q., Soares Sobrinho, J.L., Rolim Neto, P.J., Lee, P.I., et al. (2017) Enhancement of dissolution rate through eutectic mixture and solid solution of posaconazole and benznidazole. International Journal of Pharmaceutics. 525 (1), 32–42.

[27] Sarawade, P.B., Kim, J.K., Kim, H.K., and Kim, H.T. (2007) High specific surface area TEOS-based aerogels with large pore volume prepared at an ambient pressure. Applied Surface Science. 254 (2), 574–579.

[28] Rizzi, F., Castaldo, R., Latronico, T., Lasala, P., Gentile, G., Lavorgna, M., et al. (2021) High surface area mesoporous silica nanoparticles with tunable size in the sub-micrometer regime: Insights on the size and porosity control mechanisms. Molecules. 26 (14),.

[29] Tabasi, H., Mosavian, M.T.H., Darroudi, M., Khazaei, M., Hashemzadeh, A., and Sabouri, Z. (2022) Synthesis and characterization of amine-functionalized Fe3O4/Mesoporous Silica Nanoparticles (MSNs) as potential nanocarriers in drug delivery systems. Journal of Porous Materials.

[30] Lee, C.K., Chiang, A.S.T., and Tsay, C.S. (1996) The characterization of porous solids from gas adsorption measurements. Key Engineering Materials. 115 21–44.

[31] Sotomayor, F.J., Cychosz, K.A., and Thommes, M. (2018) Characterization of Micro/Mesoporous Materials by Physisorption: Concepts and Case Studies. .

[32] Karamikamkar, S., Abidli, A., Behzadfar, E., Rezaei, S., Naguib, H.E., and Park, C.B. (2019) The effect of graphene-nanoplatelets on gelation and structural integrity of a polyvinyltrimethoxysilane-based aerogel. RSC Advances. 9 (20), 11503–11520.

[33] Szekalska, M., Citkowska, A., Wróblewska, M., and Winnicka, K. (2021) The impact of gelatin on the pharmaceutical characteristics of fucoidan microspheres with posaconazole. Materials. 14 (15),.

[34] Wang, L., Zhong, Y., Qian, C., Yang, D., Nie, J., and Ma, G. (2020) A natural polymer-based porous sponge with capillary-mimicking microchannels for rapid hemostasis. Acta Biomaterialia. 114 193–205.

[35] Follmann, H.D.M., Oliveira, O.N., Lazarin-Bidóia, D., Nakamura, C. v., Huang, X., Asefa, T., et al. (2018) Multifunctional hybrid aerogels: Hyperbranched polymer-trapped mesoporous silica nanoparticles for sustained and prolonged drug release. Nanoscale. 10 (4), 1704–1715.

[36] Mercorelli, B., Luganini, A., Celegato, M., Palù, G., Gribaudo, G., Lepesheva, G.I., et al. (2020) The clinically approved antifungal drug posaconazole inhibits human cytomegalovirus replication. Antimicrobial Agents and Chemotherapy. 64 (10),.